Bioorganic Chemistry 105 (2020) 104441

Contents lists available at ScienceDirect

Bioorganic Chemistry

journal homepage: www.elsevier.com/locate/bioorg

Synthesis, biological properties, and acid dissociation constant of novel naphthoquinone–triazole hybrids

Yahya Nural [a,b,*], Sadin Ozdemir [c], Osman Doluca [d], Bunyamin Demir [b,e], Mustafa Serkan Yalcin [f], Hasan Atabey [g], Beyza Kanat [d], Selma Erat [b,h], Hayati Sari [i], Zeynel Seferoglu [j,**]

[a] Department of Analytical Chemistry, Faculty of Pharmacy, Mersin University, Mersin 33169, Turkey
[b] Advanced Technology, Research and Application Center, Mersin University, 33343 Mersin, Turkey
[c] Food Processing Programme, Technical Science Vocational School, Mersin University, Mersin 33343, Turkey
[d] Department of Biomedical Engineering, Izmir University of Economics, Izmir 35330, Turkey
[e] Department of Mechanical Engineering, Faculty of Engineering, Mersin University, Mersin 33169, Turkey
[f] Department of Chemistry and Chemical Processing Technologies, Technical Science Vocational School, Mersin University, Mersin 33343, Turkey
[g] Mersin National Education Directorate, Department of Analytical Chemistry, Mersin, Turkey
[h] Department of Medical Services and Techniques, Vocational School of Technical Sciences, Mersin University, Mersin 33343, Turkey
[i] Department of Chemistry, Faculty of Science and Arts, Tokat Gaziosmanpasa University, Tokat 60250, Turkey
[j] Department of Chemistry, Faculty of Science, Gazi University, Ankara 06500, Turkey

ARTICLE INFO

Keywords:
Naphthoquinone
Triazole
Click chemistry
DNA-binding
DNA-cleavage
Antioxidant
Antibacterial
Antifungal
Acid dissociation constants

ABSTRACT

A series of novel 1,4-naphthoquinone–triazole hybrids, *N*-(3-amino-1,4-dioxo-1,4-dihydronaphthalen-2-yl)-2-(4-R-1*H*-1,2,3-triazol-1-yl)acetamide, was synthesized by click chemistry in the presence of sodium ascorbate and copper(II) sulfate pentahydrate in 81–94% yield. Various biological properties of the synthesized compounds including DNA binding/cleavage, antioxidant, antibacterial and antifungal properties were evaluated. The DNA binding study was performed using dsDNA and G-quadruplex DNA. All of the compounds showed fluorescence increase in the presence of DNA, regardless of the structure. Up to 2.9 and 2.5 times fluorescence increase upon incubation with double stranded or G-quadruplex DNA was detected for **5f** and **5g**, respectively. The docking studies performed on dsDNA and G-quadruplex structures suggested compounds' mode of interactions were populated around the grooves. All of the compounds showed excellent DNA cleavage activity and **5e** was almost degraded the plasmid DNA. The highest radical scavenging activity was obtained as 89.9% at 200 mg/L with **5d**. However, the highest ferrous chelating activity was obtained as 68.1% at 200 mg/L with **5g**. The compounds exhibited antimicrobial activity against *Bacillus cereus*, *Legionella pneumophila* subsp. *pneumophila*, *Staphylococcus aureus*, *Pseudomonas aeruginosa*, *Escherichia coli* and *Enterococcus hirae* as bacteria strains and *Candida albicans* and *Candida tropicalis as microfungus* strains. The compounds exhibited antibacterial and antifungal activity in the range of 4–128 μg/mL and 16–128 μg/mL, respectively. The best antimicrobial activity was obtained with **5d** and **5e** with a MIC value of 4 μg/mL against *Enterococcus hirae*. The acid dissociation constants (pK_a) were determined potentiometrically in 20% (v/v) dimethyl sulfoxide-water hydro-organic solvent at an ionic background of 0.1 mol/L of NaCl, at 25 ± 0.1 °C. Five pK_a values were obtained for each ligand.

1. Introduction

Click chemistry, a term introduced by Sharpless in 2001 [1], is one of the most popular strategy for synthesis of pharmacologically active compounds. Because click chemistry offers many advantages such as stereo- and regio-specific product, high yield, mild reaction conditions etc., it has rapidly become a popular tool in drug research. Click chemistry allows the reliable synthesis of a large number of new compounds. Copper-catalyzed azide-alkyne cycloaddition click chemistry is widely used in the synthesis of 1,4-substituted-1,2,3-triazoles as regio-

* Corresponding author at: Department of Analytical Chemistry, Faculty of Pharmacy, Mersin University, Mersin 33169, Turkey.
** Corresponding author.
E-mail addresses: yahyanural@mersin.edu.tr (Y. Nural), znseferoglu@gazi.edu.tr (Z. Seferoglu).

https://doi.org/10.1016/j.bioorg.2020.104441
Received 27 July 2020; Received in revised form 17 September 2020; Accepted 27 October 2020
Available online 29 October 2020

and stereo-specific. Triazoles represent an important group of pharmacophores of drug chemistry and there are many drugs or drug candidates containing 1,2,3-triazole moiety such as Rufinamide, Savolitinib, Seviteronel, Solithromycin, Ticagrelor, Molidustat and Tazobactam in the markets (Fig. 1) [2–5].

Triazole moiety has many indispensable properties desired in drug researches such as non-toxicity, stability under physiological conditions, H-bonds and π-π stacking interactions and having both acidic and basic character [1–5]. It is known that 1,2,3-triazole-containing hybrids exhibited a wide range of pharmacological activities such as antibacterial [6–9], antimycobacterial [10], antifungal [11–13], antiviral [14], anticancer [15–17], DNA–binding [18,19], DNA–cleavage [20,21], antioxidant [22–25] and multi-target inhibitors against Alzheimer disease [25].

Naphthoquinone derivatives naturally occur in various fungi, bacteria and plants species and play an active role in various biological processes [26]. The 1,4-naphthoquinone is one of the privileged pharmacophore group in drug research since, a great number of naturally occurring compounds and many synthetic drugs such as atovaquone, buparvaquone and lapachol contain naphthoquinone core in their molecular structures (Fig. 2) [27,28]. The 1,4-naphthoquinone derivatives are known to showed a wide range of pharmacological activities, such as antibacterial [29–33], antifungal [29,34], antimalarial [35], antioxidant [36,37], anticancer [38,39], DNA–binding/cleavage [40,41] activities. The synthesis of hybrids that contain at least two pharmacophore groups is an important strategy for achieving invaluable pharmacological activities. The binding of 1,2,3-triazole core to the molecular structure of pharmacologically active compounds has become very popular in recent years [2–5]. Within this framework, there are numerous studies in medicinal chemistry on the synthesis of compounds that have both triazole and naphthoquinone moieties in their molecular structure. It has been reported that the compounds exhibited a wide range of pharmacological activities such as anticancer [42], anti-inflammatory [43] anti-*T. cruzi* [44], leishmanicidal [45] and anti-mycobacterial [46] activity. In the light of this information, it was aimed to synthesize potentially bioactive novel hybrid compounds containing naphtoquinone and 1,2,3-triazole pharmacophore groups and to investigate a wide range of biological activities. Although many compounds bearing 1,2,3-triazole and 1,4-naphtoquinone rings have been synthesized in literature, there is no hybrid similar to 1,4-naphthoquinone–-triazole hybrids to be reported in present study.

In present study, novel 1,4-naphthoquinone–1,2,3-triazole hybrids were synthesized and a wide range pharmacological activities of synthesized hybrids (DNA–binding/cleavage, antioxidant, antibacterial and antifungal properties) were reported. Additionally, acid dissociation constants (pK_a) were determined in 20% (v/v) dimethyl sulfoxide (DMSO) were also reported.

2. Experimental

2.1. Materials and instrumentation

The precursor chemicals purchased from Merck or Aldrich were high-grade and used without further purification. Fourier-transform infrared spectroscopy (FTIR) spectra were recorded by a Mattson 1000 FTIR spectrophotometer. Nuclear magnetic resonance (NMR) spectra and decoupling experiments were recorded with a Bruker Ultrashield Plus Biospin GmbHt at 400 MHz. Chemical shifts were given in parts per million (δ) downfield from TMS as internal standard. Spectra were determined in dimethyl sulfoxide-d_6. The following abbreviations were used; s = singlet, d = doublet, dd = doublet of doublets, q = quartet, t = triplet, td = triplet of doublets and m = multiplet. High resolution mass spectra (HRMS) were recorded in Waters-LCT-Premier-XE-LTOF (TOF-MS) and Agilent 6224 TOF LC-MS instruments using electrospray ionization technique and are reported in *m/z* (rel.%). Melting points were determined by a Mettler Toledo MP90 device. The pH-metric titrations were performed using a Titroline 7000 automated titrator with SI-Analytics combined with a glass pH electrode, which could be controlled by a computer and had an automatic micro-burette.

2.2. The synthesis of 2,3-diaminonaphthalene-1,4-dione, 2

The 2,3-diaminonaphthalene-1,4-dione **2** was prepared from 2,3-dichloronaphthalene-1,4-dione **1** using the method specified in literatures [47,48] and structure of the compound **2** was confirmed by ^{1}H NMR spectroscopy, which were found to be identical with the data described in Ref. [47,48].

2.3. The synthesis of N-(3-amino-1,4-dioxo-1,4-dihydronaphthalen-2-yl)-2-chloroacetamide, 3

The stirred solution of 2,3-diaminonaphthalene-1,4-dione (0.190 g, 1 mmol) in chloroform (20 mL) at 0 °C was supplemented with a solution of pyridine (0.160 g, 2 mmol) in chloroform (10 mL) and the

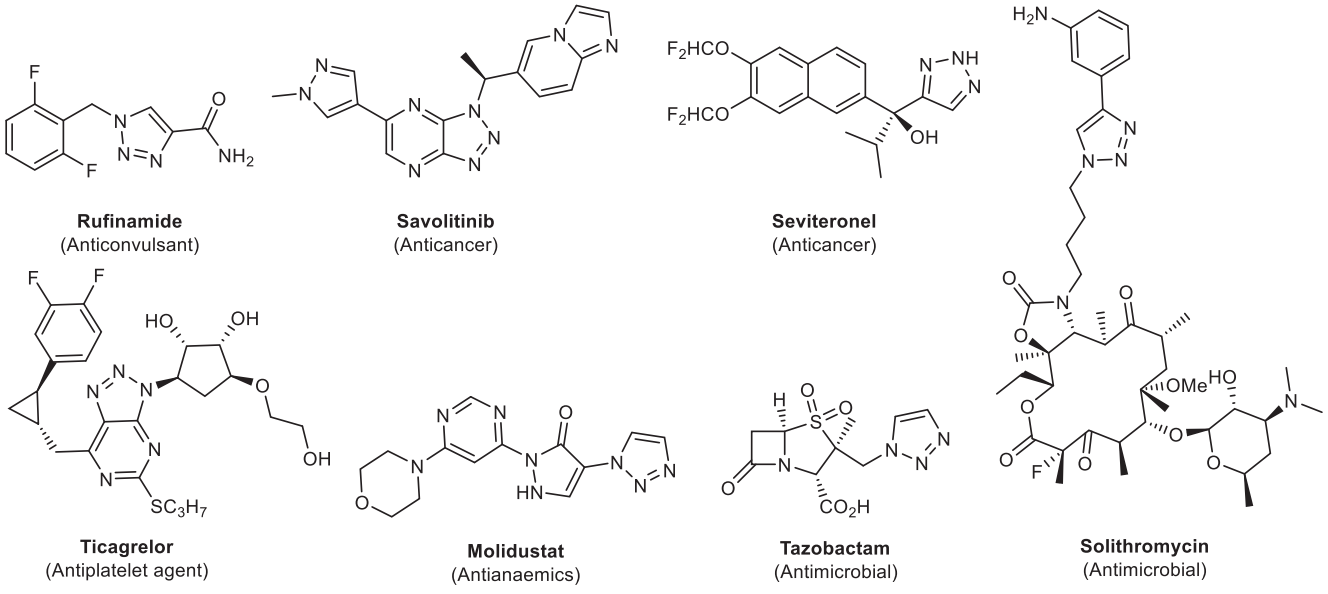

Fig. 1. Some pharmaceuticals based on 1,2,3-triazoles.

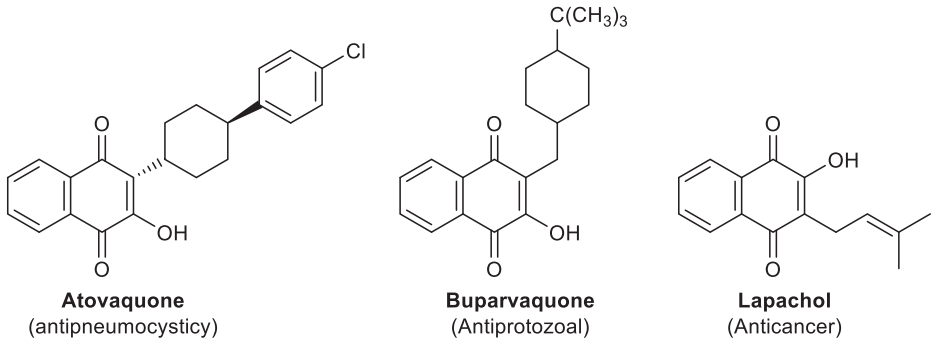

Fig. 2. Some pharmaceuticals based on naphthoquinones.

resultant mixture was stirred for 15 min. After then, a solution of chloroacetyl chloride (0.230 g, 2 mmol) in chloroform (20 mL) was added to the reaction medium and was allowed the temperature to come to room temperature. Upon completion of the reaction after 6 h, the solvent was evaporated under reduced pressure and the crude product was first washed with water and then washed several times with diethyl ether and dichloromethane (DCM), respectively, in this way the pure product was obtained as orange powder. Yield, 0.20 g, 75%. m.p.: 198–200 °C (decomp.). IR (cm^{-1}): υ_{max} 3412, 3259, 3210, 3005, 2954, 1683. ^{1}H NMR (400 MHz, DMSO-d_6): δ 9.36 (s 1H, NH), 7.99–7.95 (m, 2H, Ar-H), 7.83 (td, 1H, $J = 7.5$ Hz, 1.3 Hz, Ar-H), 7.74 (td, 1H, $J = 7.5$ Hz, 1.3 Hz, Ar-H), 6.99 (s, 2H, NH_2), 4.29 (s, 2H, CH_2). ^{13}C NMR (100 MHz, DMSO-d_6): δ 181.6 (C═O), 177.5 (C═O), 164.6 (C═O), 144.2, 134.9, 132.5, 132.2, 130.1, 125.8, 125.6, 111.7, 43.0. HRMS (ESI-TOF-MS): calcd. for $C_{12}H_9ClN_2O_3$ $[M+H]^+$ 265.0380; found 265.0371.

2.4. The synthesis of N-(3-amino-1,4-dioxo-1,4-dihydronaphthalen-2-yl)-2-azidoacetamide, **4**

The stirred solution of the compound **3** (0.270 g, 1 mmol) in dimethylformamide (DMF) (10 mL) was supplemented with a solution of sodium azide (0.100 g, 1.5 mmol) in DMF (10 mL) and the resultant mixture was stirred at 75 °C for 18 h. After completion of the reaction, the mixture was quenched with saturated aqueous sodium bicarbonate, and extracted with ethyl acetate. The crude mixture was purified by column chromatography (ethyl acetate:hexane / 1:2) to have the pure product **4** (0.220 g, 81%) as brown powder. m.p.: 192–194 °C (decomp.). IR (cm^{-1}): υ_{max} 3413, 3288, 3204, 3067, 2948, 2114, 1690. ^{1}H NMR (400 MHz, DMSO-d_6): δ 9.24 (s 1H, NH), 7.99–7.96 (m, 2H, Ar-H), 7.85–7.81 (m, 1H, Ar-H), 7.76–7.72 m, 1H, Ar-H), 7.05 (s, 2H, NH_2), 4.04 (s, 2H, CH_2). ^{13}C NMR (100 MHz, DMSO-d_6): δ 181.6 (C═O), 177.6 (C═O), 166.2 (C═O), 144.4, 134.9, 132.4, 132.2, 130.1, 125.8, 125.6, 111.6, 50.8. HRMS (ESI-TOF-MS): calcd. for $C_{12}H_9N_5O_3$ $[M+H]^+$ 272.0785; 272.0784.

2.5. General procedure for the synthesis of 1,4-naphthoquinone–triazole hybrids, **5a–h**

The novel 1,4-naphthoquinone–triazole hybrids **5a–h** were synthesized by click chemistry. The stirred solution of the compound **4** (1 mmol) in DMF (20 mL) was supplemented with sodium ascorbate (0.6 mmol), $CuSO_4{\cdot}5H_2O$ (0.3 mmol), corresponding alkyne compound (1.5 mmol) and 4 mL deionized water, respectively. Resultant mixture was stirred at room temperature for 16 h and then, the mixture was quenched with saturated aqueous sodium bicarbonate, and extracted with ethyl acetate. The crude product was purified by column chromatography (ethyl acetate:hexane / 1:2).

2.5.1. N-(3-amino-1,4-dioxo-1,4-dihydronaphthalen-2-yl)-2-(4-(pentan-2-yl)-1H-1,2,3-triazol-1-yl)acetamide, **5a**

Black powder. Yield, 0.33 g, 89%. m.p.: 172–174 °C. IR (cm^{-1}): υ_{max} 3424, 3309, 3255, 3066, 2956, 2931, 1689, 1663, 1614. ^{1}H NMR (400 MHz, DMSO-d_6): δ 9.54 (s 1H, NH), 7.99–7.96 (m, 2H, Ar-H), 7.85–7.81 (m, 2H, Ar-H and triazole C—H), 7.74 (td, 1H, $J = 7.5$ Hz, 0.7 Hz, Ar-H), 7.05 (s, 2H, NH_2), 5.28 (s, 2H, $C(O)CH_2$), 290–2.85 (m, 1H, C2H), 1.66–1.57 (m, 1H, C3H), 1.53–1.44 (m, 1H, C4H), 1.30–1.20 (m, 2H, C3-H′, C4H′), 1.21 (d, 3H, $J = 7.3$ Hz, $C1H_3$), 0.86 (t, 3H, $J = 7.3$ Hz, $C5H_3$). ^{13}C NMR (100 MHz, DMSO-d_6): δ 181.5 (C═O), 134.8, 132.4, 132.1, 130.0, 125.7, 125.5, 122.2, 51.6, 38.7, 30.0, 20.4, 19.6, 13.8. HRMS (ESI-TOF-MS): calcd. for $C_{19}H_{21}N_5O_3$ $[M+H]^+$ 368.1723; found 368.1711.

2.5.2. N-(3-amino-1,4-dioxo-1,4-dihydronaphthalen-2-yl)-2-(4-cyclopropyl-1H-1,2,3-triazol-1-yl)acetamide, **5b**

Orange powder. Yield, 0.31 g, 91%. m.p.: 230–232 °C (decomp.). IR (cm^{-1}): υ_{max} 3354, 3263, 3211, 3143, 3071, 3005, 2950, 1670, 1613. ^{1}H NMR (400 MHz, DMSO-d_6): δ 9.53 (s 1H, NH), 7.99–7.96 (m, 2H, Ar-H), 7.86–7.80 (m, 2H, Ar-H and triazole C—H), 7.73 (td, 1H, $J = 7.5$ Hz, 0.8 Hz, Ar-H), 7.04 (s, 2H, NH_2), 5.26 (s, 2H, $C(O)CH_2$), 1.99–1.93 (m, 1H, C1H), 0.92–0.88 (m, 2H, C2H, C3H), 0.74–0.70 (m, 2H, C2H′, C3H′). ^{13}C NMR (100 MHz, DMSO-d_6): δ 181.5 (C═O), 177.5 (C═O), 164.2 (C═O), 148.6, 144.3, 134.8, 132.4, 132.1, 130.0, 125.7, 125.5, 122.1, 111.4, 51.6, 7.4 (2 × C), 6.4. HRMS (ESI-TOF-MS): calcd. for $C_{17}H_{15}N_5O_3$ $[M+H]^+$ 338.1253; found 338.1245.

2.5.3. N-(3-amino-1,4-dioxo-1,4-dihydronaphthalen-2-yl)-2-(4-cyclopentyl-1H-1,2,3-triazol-1-yl)acetamide, **5c**

Green powder. Yield, 0.32 g, 86%. m.p.: 246–248 °C (decomp.). IR (cm^{-1}): υ_{max} 3458, 3347, 3280, 3115, 3067, 2950, 2867, 1688, 1666, 1628. ^{1}H NMR (400 MHz, DMSO-d_6): δ 9.55 (s 1H, NH), 7.99–7.94 (m, 2H, Ar-H), 7.85–7.79 (m, 2H, Ar-H and triazole C—H), 7.75–7.72 (m, 1H, Ar-H), 7.07 (s, 2H, NH_2), 5.28 (s, 2H, $C(O)CH_2$), 3.18–3.06 (m, 1H, C1H), 2.06–1.94 (m, 2H, C2H, C5H), 1.70–1.56 (m, 6H, C2H′, C3H, C3H′, C4H, C4H′ C5H′). ^{13}C NMR (100 MHz, DMSO-d_6): δ 181.5 (C═O), 177.5 (C═O), 164.2 (C═O), 144.3, 134.8, 132.4, 132.1, 130.0, 125.7, 125.5, 122.2, 111.5, 51.6, 36.1, 32.7 (2 × C), 24.6 (2 × C). HRMS (ESI-TOF-MS): calcd. for $C_{19}H_{19}N_5O_3$ $[M+H]^+$ 366.1566; found 366.1550.

2.5.4. N-(3-amino-1,4-dioxo-1,4-dihydronaphthalen-2-yl)-2-(4-(cyclohexylmethyl)-1H-1,2,3-triazol-1-yl)acetamide, **5d**

Green powder. Yield, 0.37 g, 94%. m.p.: 202–204 °C (decomp.). IR (cm^{-1}): υ_{max} 3465, 3356, 3281, 3109, 3062, 2925, 2852, 1688, 1669, 1625. ^{1}H NMR (400 MHz, DMSO-d_6): δ 9.55 (s 1H, NH), 8.03–7.93 (m, 2H, Ar-H), 7.85–7.81 (m, 2H, Ar-H and triazole C—H), 7.75–7.72 (m, 1H, Ar-H), 7.06 (s, 2H, NH_2), 5.29 (s, 2H, $C(O)CH_2$), 2.57–2.45 (m, 2H, C1H, C1H′), 1.65–1.53 (m, 6H, C2H, C3H, C4H, C5H, C6H, C7H), 1.23–1.06 (m, 3H, C4H′, C5H′, C6H′), 0.97–0.86 (m, 2H, C3H′, C7H′). ^{13}C NMR (100 MHz, DMSO-d_6): δ 181.6 (C═O), 177.6 (C═O), 164.3 (C═O), 144.3, 134.9, 132.5, 132.2, 130.1, 125.8, 125.6, 123.9, 123.8, 111.5, 51.6, 37.6, 32.7, 32.4 (2 × C), 26.0, 25.6 (2 × C). HRMS (ESI-TOF-MS): calcd. for $C_{21}H_{23}N_5O_3$ $[M+H]^+$ 394.1879; found 394.1869.

2.5.5. N-(3-amino-1,4-dioxo-1,4-dihydronaphthalen-2-yl)-2-(4-(2-bromoethyl)-1H-1,2,3-triazol-1-yl)acetamide, ***5e***

Brown powder. Yield, 0.36 g, 88%. m.p.: 182–184 °C (decomp.). IR (cm^{-1}): υ_{max} 3320, 3232, 3168, 3017, 2966, 1686, 1646, 1618. ^{1}H NMR (400 MHz, DMSO-d_6): δ 9.57 (s 1H, NH), 7.99–7.96 (m, 3H, Ar-H and triazole C—H), 7.85–7.81 (m, 1H, Ar-H), 7.75–7.72 (m, 1H, Ar-H), 7.05 (s, 2H, NH_2), 5.33 (s, 2H, C(O)CH_2), 3.75 (t, 2H, J = 6.5 Hz, CH_2), 3.23 (t, 2H, J = 6.5 Hz, CH_2). ^{13}C NMR (100 MHz, DMSO-d_6): δ 181.5 (C═O), 177.6 (C═O), 164.1 (C═O), 144.3, 134.9, 132.5, 132.2, 130.1, 125.8, 125.6, 124.3, 124.2, 111.5, 51.7, 32.6, 29.0. HRMS (ESI-TOF-MS): calcd. for $C_{16}H_{14}BrN_5O_3$ $[M+H]^+$ 404.0358; found 404.0344.

2.5.6. Ethyl 1-(2-((3-amino-1,4-dioxo-1,4-dihydronaphthalen-2-yl) amino)-2-oxoethyl)-1H-1,2,3-triazole-4-carboxylate, ***5f***

Brown powder. Yield, 0.32 g, 85%. m.p.: 162–164 °C (decomp.). IR (cm^{-1}): υ_{max} 3459, 3383, 3241, 3149, 3016, 2969, 1712, 1673, 1641, 1621. ^{1}H NMR (400 MHz, DMSO-d_6): δ 9.66 (s 1H, NH), 8.72 (s, 1H, triazole C—H), 7.99–7.97 (m, 2H, Ar-H), 7.85–7.81 (m, 1H, Ar-H), 7.76–7.72 (m, 1H, Ar-H), 7.08 (s, 2H, NH_2), 5.43 (s, 2H, C(O)CH_2), 4.32 (q, 2H, J = 6.9 Hz, CH_2), 1.31 (t, 3H, J = 6.9 Hz, CH_3). ^{13}C NMR (100 MHz, DMSO-d_6): δ 181.5 (C═O), 177.5 (C═O), 163.6 (C═O), 160.2 (C═O), 144.3, 138.6, 134.8, 132.4, 132.1, 130.5, 130.0, 125.7, 125.5, 111.2, 60.4, 51.9, 14.1. HRMS (ESI-TOF-MS): calcd. for $C_{17}H_{15}N_5O_5$ $[M+H]^+$ 370.1151; found 370.1143.

2.5.7. N-(3-amino-1,4-dioxo-1,4-dihydronaphthalen-2-yl)-2-(4-phenyl-1H-1,2,3-triazol-1-yl)acetamide, ***5g***

Green powder. Yield, 0.30 g, 81%. m.p.: 164–166 °C (decomp.). IR (cm^{-1}): υ_{max} 3456, 3349, 3274, 3131, 3066, 2956, 1687, 1668, 1624. ^{1}H NMR (400 MHz, DMSO-d_6): δ 9.62 (s 1H, NH), 8.55 (s, 1H, triazole C—H), 7.99–7.97 (m, 2H, Ar-H), 7.88–7.81 (m, 2H, Ar-H), 7.83 (td, 1H, J = 7.6 Hz, 0.7 Hz, Ar-H), 7.73 (td, 1H, J = 7.6 Hz, 0.7 Hz, Ar-H), 7.48–7.44 (m, 2H, Ar-H), 7.36–7.32 (m, 1H, Ar-H), 7.09 (s, 2H, NH_2), 5.42 (s, 2H, C(O)CH_2). ^{13}C NMR (100 MHz, DMSO-d_6): δ 181.6 (C═O), 177.6 (C═O), 164.1 (C═O), 146.2, 144.4, 134.9, 132.5, 132.2, 130.8, 130.1, 128.9 (2 × C), 127.8, 125.8, 125.6, 125.1 (2 × C), 122.9, 111.5, 51.9. HRMS (ESI-TOF-MS): calcd. for $C_{20}H_{15}N_5O_3$ $[M+H]^+$ 374.1253; found 374.1262.

2.5.8. N-(3-amino-1,4-dioxo-1,4-dihydronaphthalen-2-yl)-2-(4-phenethyl-1H-1,2,3-triazol-1-yl)acetamide, ***5h***

Brown powder. Yield, 0.33 g, 82%. m.p.: 177–179 °C (decomp.). IR (cm^{-1}): υ_{max} 3365, 3207, 3154, 3025, 2953, 1695, 1668, 1639, 1615. ^{1}H NMR (400 MHz, DMSO-d_6): δ 9.54 (s 1H, NH), 7.99–7.97 (m, 2H, Ar-H), 7.85–7.81 (m, 2H, Ar-H and triazole C—H), 7.75–7.72 (m, 1H, Ar-H), 7.30–7.24 (m, 4H, Ar-H), 7.20–7.16 (m, 1H, Ar-H), 7.05 (s, 2H, NH_2), 5.29 (s, 2H, C(O)CH_2), 2.94 (s, 4H, 2 × CH_2). ^{13}C NMR (100 MHz, DMSO-d_6): δ 181.6 (C═O), 177.6 (C═O), 164.3 (C═O), 144.3, 141.2, 134.9, 132.5, 132.2, 130.1, 128.30 (2 × C), 128.27 (2 × C), 125.9, 125.8, 125.6, 123.6, 123.5, 111.6, 51.7, 34.9, 27.0 HRMS (ESI-TOF-MS): calcd. for $C_{22}H_{19}N_5O_3$ $[M+H]^+$ 402.1566; found 402.1559.

2.6. DNA binding

Double stranded DNA structure (dsDNA) was prepared by mixing 5′–GACGTGTCGAAAGAGCTCCGATTA–3′ and 5′–TAATCGGAGCTCTT TCGACACGTC–3′ oligonucleotides in Tris HCl buffer (pH 7.4). The mixture was heated up to 50 °C and left to cool down to room temperature. For G-quadruplexes, 5′–AGGGTTAGGGTTAGGGTTAGGG–3′ oligonucleotide was incubated in Tris HCl buffer containing 50 mM KCl. G-quadruplexes were heated up to 95 °C and left to cool down to room temperature before use. The stock solutions containing DNA solutions were prepared at 50 μM.

The samples for fluorescence measurement were prepared for each compound at 10 μM in Tris HCl (pH 7.4) containing 5% DMSO. The DNA stock solutions were added to the sample to achieve respective equivalent concentrations. For all titrations, up to three consecutive fluorescence measurements were performed with 15 min intervals. Only the measurements after the fluorescence reached equilibrium were taken into account.

All fluorescence measurements were performed at 360 nm excitation and emissions between 380 and 700 nm with 10 nm excitation and emission slits using Jasco FP8300 in quartz cuvettes.

Docking studies of the compounds with DNA structures associated topologies were performed using Autodock Vina and in-house Python script to automate the process. To represent the dsDNA and the G-quadruplex, PDB files with accession numbers, 1BNA and 1XAV were used, respectively. After removal of water molecules, removal of non-polar hydrogens and calculation of Kollman charges, the PDB files were saved as PDBQT. Docking studies were performed with a grid size of 26 Å for all axes and centred at coordinates 0,0,0 for 1BNA and with a grid of 18, 18 and 40 Å for ×, y and z axes and centred at coordinates 14.78, 20.976 and 8.807 for 1XAV. The exhaustiveness was set to 64. Docking studies were performed on a workstation with 32 cores and 128 GB ECC Ram.

2.7. DNA cleavage activity

The DNA cleavage activity was tested by agarose gel electrophoresis, which was studied by incubation at 37 °C as follows: pBR322DNA (0.1 μg/μL) in Tris–HCl 50 mM and NaCl buffer (18 mM; pH:7.2) was reacted with 1,4-naphthoquinone–triazole hybrids **5a–h** and then the mixture was incubated for 2 h. After that the samples were electrophoresed for 120 min at 80 V in 0.9% agarose gel and Tris-boric acid-EDTA buffer. After 120 min electrophoresis, bands were monitored under UV-A light and photographed [49].

2.8. DPPH scavenging activity

DPPH radical scavenging activities of the 1,4-naphthoquinone–-triazole hybrids **5a–h** were performed according to the Blois method [50]. For this test, 2 mL of 0.004% DPPH solution was taken to each tube and then 0.5 mL of **5a–h** was added into each tube. The tubes were shaken quickly and kept at room temperature for 30 min in the dark for incubation. After incubation, absorbances were then measured at 517 nm. The ability to scavenge DPPH free radical was calculated by the following equation:

$$\%\text{Inhibition Activity} = [(A_0 - A_1)/A_0] \times 100$$

A_0 = Control absorbance and A_1 = the absorbance value of the solution containing compounds and DPPH after 30 min. The IC50 values were calculated using linear regression analysis and used to indicate antioxidant capacity.

2.9. Chelating activity

The iron chelating activities of the 1,4-naphthoquinone–triazole hybrid compounds **5a–h** were determined with the method specified by Dinis et al. [51]. Different concentrations of **5a–h** solutions were separately put into the test tubes and $FeCl_2$ (0.05 mL of 2 mM) solution was added to each tubes. The reaction was started by adding 0.1 mL of 5 mM ferrozine ($C_{20}H_{13}N_4NaO_6S_2$). After the total volume was completed to 2.5 mL with the solvent used, the solution was mixed quickly and kept for 10 min at room temperature. Then absorbance values were read at 562 nm. Without adding **5a–h**, 50 μL $FeCl_2$ (2 mM) and 2.35 mL solvent were added to 100 μL of ferrozine (5 mM) and measured spectrophotometrically at 562 nm. For blanc, 0.05 mL of $FeCl_2$ was added and final volume was completed to 2.5 mL with solvent. The same procedures were applied for the standard (EDTA). The chelating activity of the compounds for Fe^{2+} was calculated using the following equation:

$$\text{Chelating activity}(\%) = [(A_{\text{control}} - A_{\text{sample}})/A_{\text{control}}] \times 100;$$

where; $A_{control}$ is the absorbance of the control reaction, and A_{sample} represents the absorbance obtained in the presence of compounds or EDTA. In addition, IC50 values were calculated using linear regression analysis to determine iron chelating ability.

2.10. Antimicrobial activity

Six different bacteria (*Bacillus cereus*, *Legionella pneumophila* subsp. *pneumophila* (ATCC 33152), *Staphylococcus aureus* (ATCC 6538), *Pseudomonas aeruginosa* (ATCC 9027), *Escherichia coli* (ATCC 10536) and *Enterococcus hirae* (ATCC 10541)) and two microfungus (*Candida albicans* and *Candida tropicalis* (ATCC 750)) were used to investigate antimicrobial activity. The minimum inhibition concentrations (MICs) of the tested compounds were evaluated by two-fold serial dilution method. Microorganisms (about 10^8–10^9 colony forming units (CFU/mL) were inoculated in medium containing different concentrations of **5a–h**. Culture media were then incubated at 37 °C and 120 rpm for 24 h in a shaker [52].

2.11. Determination of acid dissociation constants

The pH values were measured by model TitroLine® 7000 automatic titrator using a combined glass electrode. The glass electrode was calibrated using standard buffer solutions of pH 4.01, pH 7.00 and pH 10.01 according to the procedure described elsewhere [53,54] and determination of pK_a values was performed by modification of a literature method [55,56]. To maintain the ionic strength at a desired value a high concentrated solution of NaCl was used for all titrations. Potentiometric titrations were performed in a double-walled glass titration cell at 25.0 ± 0.1 °C using a thermostat and the titration cell was stirred at a constant rate throughout the titration using a magnetic stirrer. The ligand **5a–h** solutions were prepared as 1.10^{-3} mol/L in DMSO, and 0.025 mol/L NaOH, 0.1 mol/L HCl and 1.0 mol/L NaCl stock solutions were prepared in deionized water. To determine the pK_a values of **5a–h** in 20% (v/v) DMSO-water hydro-organic solvent, titration cell was supplemented with 10 mL of the **5a–h** ligand solutions, 1 mL of the HCl solution and 5 mL of the NaCl solution from previously prepared stock solutions. After that, the titration cell was filled to 50.00 mL with deionized water, The pK_w value, which is defined as –log[H^+][OH^-] for the aqueous system, was obtained as 14.49 ± 0.07 at the ionic strength employed. The pK_a values of **5a–h** were calculated from the potentiometric data using HYPERQUAD.

3. Results and discussion

3.1. Synthesis and characterization

The synthesis of 1,4-naphthoquinone–triazole hybrids **5a–h** was performed by click chemistry in the presence of copper(II) sulfate pentahydrate and sodium ascorbate as catalyst in 81–94% yield. The 2,3-diaminonaphthalene-1,4-dione **2** was prepared from 2,3-dichloronaphthalene-1,4-dione **1** according to a literature method [47,48]. The 2,3-diaminonaphthalene-1,4-dione **2** was reacted with chloroacetyl chloride, then the resultant product **3** was reacted with sodium azide to prepare the desired intermediate **4**, *N*-(3-amino-1,4-dioxo-1,4-dihydronaphthalen-2-yl)-2-azidoacetamide. To obtain the targeted products **5a–h**, the *N*-(3-amino-1,4-dioxo-1,4-dihydronaphthalen-2-yl)-2-azidoacetamide **4** was reacted with various alkyne compounds in the presence of sodium ascorbate (0.6 equivalent) and $CuSO_4{\cdot}5H_2O$ (0.3 equivalent) in DMF / water (5:1 v/v) at room temperature [17]. **5a–h** were obtained with a good to excellent yield (81–94%) after isolation using flash chromatography (Scheme 1). The structures of **5a–h** were fully characterized by various analytical techniques such as ^{1}H NMR, ^{13}C NMR, DEPT, COSY, HMQC, FT-IR and HRMS (See supplementary part). In the FT-IR spectra of **5a–h,** after formation of the triazole ring in the 1,4-naphthoquinone–triazole hybrids **5a–h**, the characteristic strong band of the azide group of the intermediate compound **3**, which appeared at 2114 cm^{-1}, disappeared. In the ^{1}H NMR spectra of **5a–h**, proton of the triazole ring were observed as a singlet in the range of 8.72 –7.79 ppm depending on inductive effect. In the ^{1}H NMR spectra of compound **4**, the signal observed as singlet at 4.04 ppm was assigned to the protons of C(O)CH_2 group. After formation of the triazole ring, in the ^{1}H NMR spectra of **5a–h**, the corresponding signal was observed as singlet in the range of 5.43–5.26 ppm. In the ^{13}C NMR spectra of **5a–h**, although the NMR solution was prepared as very concentrated and the NMR measurement time was extended, the carbon peak belonging to the quaternary carbon atom in the triazole ring was sometimes observed in the NMR spectrum and sometimes not observed. In the ^{13}C NMR spectra of

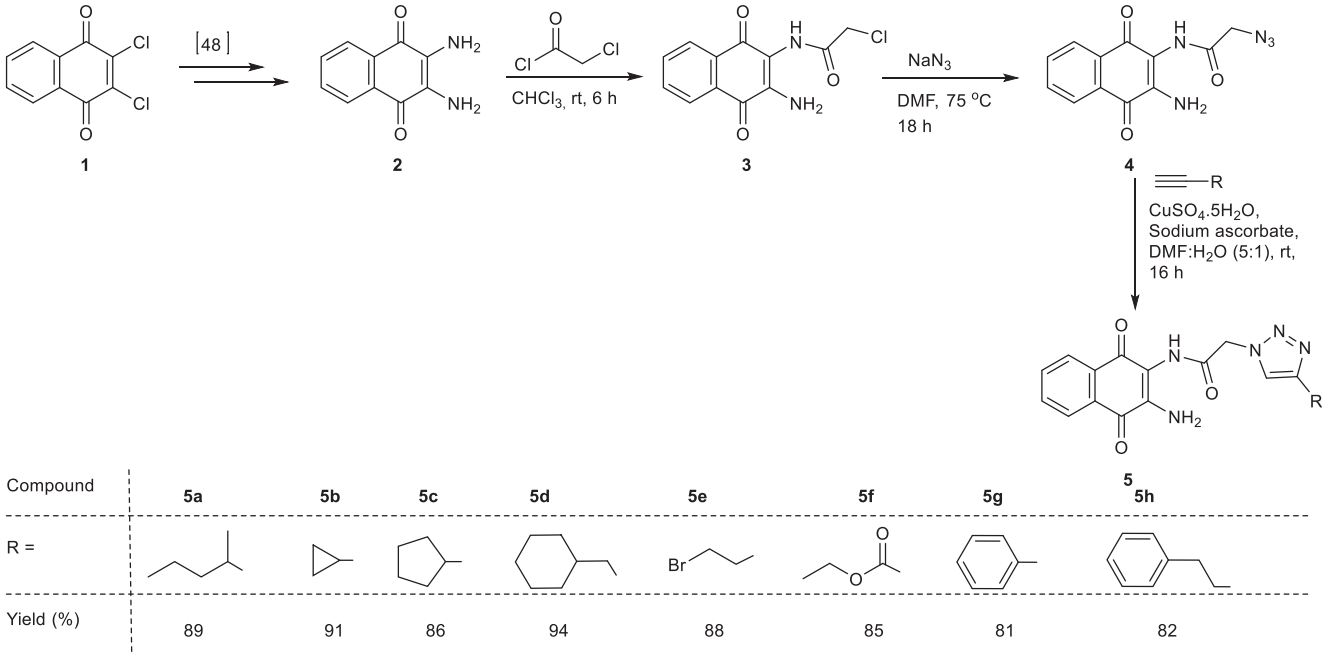

Scheme 1. Synthesis of the naphthoquinone–triazole hybrids **5a–h.**

5a, some of the C=O peaks were by no means observed. The shift values of the all carbon peaks originating from alkyne compounds have been found to be appropriate.

3.2. DNA binding activity

The potential of **5a–h** as DNA-binding fluorescent agents were analyzed through fluorescence change in the presence of dsDNA and G-quadruplex DNA. While all components showed absorbance at low wavelengths, the emission maxima varied between 400 and 440 depending on the compound. While all compounds showed very low fluorescence, an increase in fluorescence was apparent for all compounds, except for **5b** (Fig. S65). The fluorescence increase was most dramatic for **5f**, **5g** and **5h**. For these compounds, the titrations of dsDNA and G-quadruplex resulted in an increase in fluorescence (Fig. S66). Surprisingly, a shift in the emission maxima was apparent only for **5g** in the presence of dsDNA with a new maximum at 450 nm. The increase in intensity was tested up to 1:10 equivalent for dsDNA and 3:40 equivalent for G-quadruplex. The most dramatic increases in fluorescence emission in the presence of dsDNA was detected for **5f**, and in the presence of G-quadruplex it was detected for **5g** with up to 2.9 and 2.5 times increase, respectively. While all three compounds, showed fluorescence increase for the both DNA topologies, **5g** showed the highest difference in fluorescence emission in the presence of difference DNA-topologies as it showed a fluorescence increase of only 1.3 times increase for equal amount of dsDNA in comparison to G-quadruplex. This could be interpreted as **5g** having higher potential as a topology specific fluorescent probe among the compounds tested.

The docking studies have showed that affinity of the compounds varied between −7.0 and −8.3 kcal/mol for G-quadruplex topology, 1XAV (Table S1). For all fluorescently active compounds, **5f–h**, grooves of the G-quadruplex remained as the main target (Figure S67.d-f). Docking positions also revealed formation of hydrogen bonds by all compounds and it may be associated to change in fluorescence properties in the presence of DNA structures (Table S2). In the case of duplex DNA, higher affinities were observed in general and minor groove was determined as the only target by the docking studies (Figure S67.a-c). For all compounds, the affinities towards the duplex form of DNA have ranged between −8.5 and −10.8 kcal/mol. In all cases, the highest affinities for both DNA structures belonged to **5g**. Subsequently, a dramatic increase in fluorescence was detected in both dsDNA and G-quadruplex of **5g**.

3.3. DNA cleavage activity

The DNA cleavage activity of **5a–h** was performed by agarose gel electrophoresis. DNA cleavage was examined by relaxation of super coiled circular form into nicked circular form and linear form. When circular DNA is run to electrophoresis, relatively fast move will be monitored for the uncleaved super coiled form. If one strand cleavage is observed, the super coiled form relax to generate slower moving open circular form. If double strand cleavage is occurred, linear form produces and moves between super coiled and open circular forms. The results of DNA cleavage activity of **5a–h** are presented in Fig. 3. After the gel electrophoresis, it can clearly be seen in Fig. 3 that all tested compounds **5a–h** exhibited nuclease activity, whereas DNA + DMSO did not exhibit cleavage activity in Lane 2. The compound **5a** (Lane 3) showed single strand cleaved DNA activity, whereas **5b**, **5f** and **5g** demonstrated double strand cleaved DNA activities in Lane 4 Lane 6 and Lane 8, respectively. Among the test compounds, especially **5c**, **5d**, **5e** and **5h** showed excellent cleaved DNA activities in Lane 5, Lane 7, Lane 9 and Lane 10, respectively. The plasmid DNA was cleaved into the unidentified small DNA fragments with **5c**, **5d** and **5h**. And also, **5e** was nearly degraded the plasmid DNA into the indistinguishable particles. As a result, the 1,4-naphthoquinone-triazole hybrids **5a–h** may be applied in medicine industries after further studies.

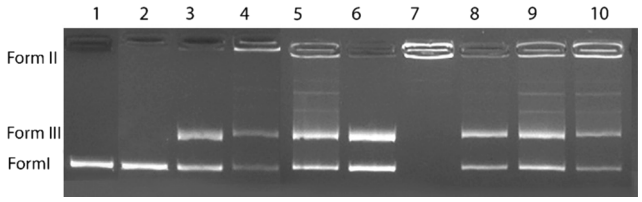

Fig. 3. DNA cleavage activities of the compounds **5a–h**. Lane 1, pBR 322 DNA; Lane 2, pBR 322 DNA + DMSO; Lane 3, pBR 322 DNA + 250 μg/mL of **5a**; Lane 4, pBR 322 DNA + 250 μg/mL of **5b**; Lane 5, pBR 322 DNA + 250 μg/mL of **5c**; Lane 6, pBR 322 DNA + 250 μg/mL of **5g**; Lane 7 pBR 322 DNA + 250 μg/mL of **5e**; Lane 8, pBR 322 DNA + 250 μg/mL of **5f**; Lane 9, pBR 322 DNA + 250 μg/mL of **5d**; Lane 10, pBR 322 DNA + 250 μg/mL of **5h.**

3.4. DPPH scavenging and chelating activity

The antioxidant activities of 1,4-naphthoquinone-triazole hybrids **5a–h** were determined using 2,2-diphenyl-1-picrylhydrazyl (DPPH) free radical. The DPPH process is one of the most powerful procedures for measuring the quantity of radical scavenging compounds active by chain-breaking operations [57]. DPPH scavenging activity measurement is also a fast, easy, economic and suitable method to check the antioxidant activity of the compounds. Fig. 4 is depicted the radical scavenging ability of **5a–h**, compared with Trolox and Ascorbic acids. All tested compounds exhibited well scavenging radical ability. As seen in Fig. 4, the radical scavenging activities were concentration dependent. When the concentration of **5a**, **5b**, **5c**, **5d**, **5e**, **5f**, **5g** and **5h** was increased from 25 mg/L to 50 mg/L, the scavenging activities were increased from 27.1% to 30.1%, from 31.4% to 59.9%, from 30.6% to 36.8%, from 41.8% to 53.4%, from 29.6% to 52.9%, from 33.5% to 47.6%, from 26.2% to 39.1%, and from 32.9% to 37.6%, respectively. The DPPH scavenging activities at 100 mg/L of **5b**, **5d**, **5e**, **5f**, and **5h** were obtained as 75.6%, 83.7%, 61.1%, 59.4%, and 49.8%, respectively. The highest scavenging activity was obtained as 89.9% at 200 mg/L with **5d**. Additionally, IC50 values of **5a**, **5b**, **5c**, **5d**, **5e**, **5f**, **5g** and **5h** were determined as 223.6 mg/L, 48.9 mg/L, 89.2 mg/L, 40.4 mg/L, 47.9 mg/L, 77.9 mg/L, 125.8 mg/L and 107.2 mg/L, respectively. The antioxidant abilities of the compounds **5a–h** may be due to their redox characteristics, which give them to treat as reducing agents or H^+ donor and free radical scavengers. These results showed that the synthesized compounds may be better candidate for the future studies to develop new antioxidant agents.

Ferrous Chelating Activity: Most of the reactive oxygen species (ROS) are created as by-product throughout the electron transport system and other metabolic activities and ROS are also generated by metal catalyzed oxidation reactions. The transition metal Fe(II) ions have the ability to maintain the generation of free radicals by loss or gain of electrons. So, the reducing of the generation of ROS can be achieved by the chelation of toxic metal ions with chelating agents [58]. The **5a–h** have been

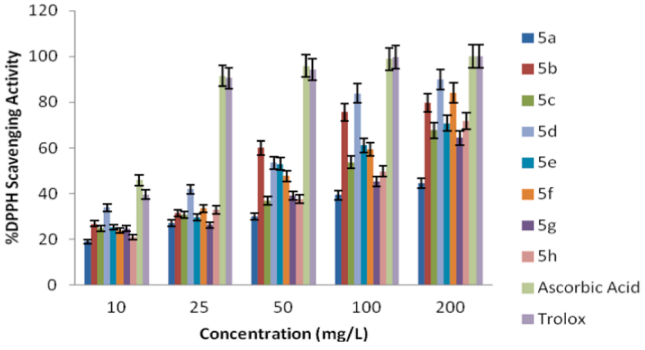

Fig. 4. % Radical scavenging activity of the 1,4-naphthoquinone-triazole hybrids **5a–h.**

tested for their ferrous chelating activities. The ferrous chelating assay of the compounds **5a–h** indicated that all compounds **5a–h** exhibited chelating activities and as presented in Fig. 5, chelating activities were concentration dependent. Chelating activity of **5a–h** was compared with the standard (EDTA) material. The ferrous chelating activities at 25 mg/L were obtained as 26.1%, 18.8%, 24.3%, 24.7%, 22.6%, 30.1%, 26.4%, and 21.1% for **5a**, **5b**, **5c**, **5d**, **5e**, **5f**, **5g** and **5h**, respectively. The ferrous chelating method displayed that the compounds **5a–h** also exhibited chelating ability in the order of **5g** > **5f** > **5a** > **5c** > **5e** > **5b** > **5d** > **5h** at concentration of 100 mg/L. The highest ferrous chelating activity was obtained as 68.1% with **5g** at concentration of 200 mg/L. Moreover, the IC50 values of **5a**, **5b**, **5c**, **5d**, **5e**, **5f**, **5g** and **5h** were found as 153.2 mg/L, 163.7 mg/L, 169.6 mg/L, 308.1 mg/L, 136.4 mg/L, 130.4 mg/L, 121.8 mg/L and 710.9 mg/L, respectively. The chelating agents are used for neutralizing iron overload in the body in chelation therapy for treatment of several diseases such as Alzheimer, Parkinson, Thalassemia [59,60]. According to present findings, especially **5e**, **5f** and **5g** can be used in chelation therapy after further investigations.

3.5. Antimicrobial activities

The increase of antibiotic tolerance in microorganisms especially bacteria has become a significant attention for successful treatment and diagnosis of infectious illnesses. Over the past few decades, major investigations have been realized on the synthesis and development of new medicines for combating multi-drug tolerance in microorganisms [61]. The results of the antimicrobial activity of **5a–h** and standard antibiotics are demonstrated in Table 1. All compounds tested **5a–h** exhibited antimicrobial activity against all tested microorganisms with MICs ranging between 4 and 128 μg/mL. Only one substituent has been changed in the molecular structure of the 1,4-naphthoquinone-triazole hybrids **5a–h**. Compound **5b**, which contains the cyclopropyl group as a substituent, exhibited the best activity among the others against *E. coli* and *S. aureus* with a MIC value of 16 μg/mL and 8 μg/mL, respectively. Compared to ampicillin (MIC value = 0.5 μg/mL and 1 μg/mL, respectively), all compounds showed moderate antibacterial activity against *E. coli* but **5b** showed noteworthy antibacterial activity against *S. aureus*. The **5d**, which contains the cyclohexylmethyl group as a substituent, and **5b** exhibited the best activity among the others against *B. cereus* and *P. aeruginosa* with a MIC value of 8 μg/mL. Compared to ampicillin (MIC value = 1 μg/mL, 0.5 μg/mL, respectively), **5b** and **5d** exhibited remarkable antibacterial activity against *B. cereus*. All compounds exhibited antibacterial activity against *L. pneumophila* subsp. *pneumophila* with a MIC value in the range of 16–64 μg/mL. The **5e**, which contains the 2-bromoethyl as a substituent, and **5d** exhibited better antibacterial activity against *E. hirae* with a MIC value of 4 μg/mL and *E. hirae* was the most sensitive microorganism among the test compounds. Compound **5d** exhibited the best antifungal activity among the others against *C. albicans* and *C. tropicalis* with a MIC value of 32 μg/mL and 16 μg/mL, respectively. Compared to Fluconazole (MIC value = 0.5 μg/mL), **5a–h** exhibited moderate antifungal activity against the tested fungus strains. As a result of antimicrobial activity study, it was observed that especially **5d** could be an important antimicrobial agent after some modifications to its molecular structure.

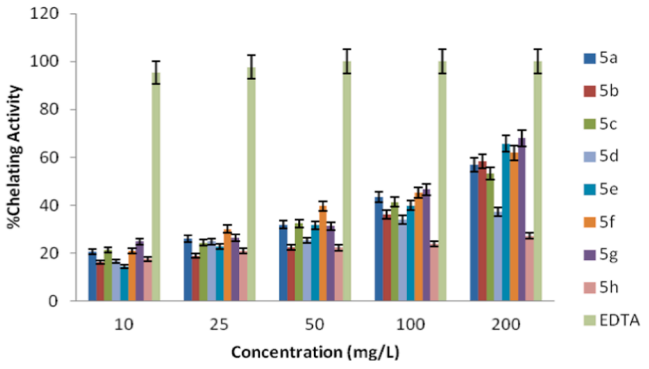

Fig. 5. Chelating activity of the 1,4-naphthoquinone-triazole hybrids **5a–h.**

3.6. Acid dissociation constants

In order to continue drug research studies on a molecule, pK_a value (s) which is one of the most important physicochemical parameters must be determined because it provides critical data related to acidity, degree of ionization, solubility and hydrogen bonding capacity of the compounds [62,63]. The pK_a values of **5a–h** were determined potentiometrically at 25.0 ± 0.1 °C, 0.1 mol / L ionic strength of NaCl in 20% (v/v) DMSO-water hydro-organic solvent system using a literature method [54,55]. The calculated pK_a values are given in Table 2, and titration curves of the ligands **5a–h** and distribution curve of **5a** for symbolized all ligands **5a–h** are presented in Fig. 6. All obtained logβ values and distribution curves were submitted as supporting data (Fig. S68).

According to the results, five protonated species were obtained as LH, LH_2, LH_3, LH_4 and LH_5 calculated five pK_a values. Full protonated form of the ligands is showed in Fig. 7 and four protonated species are related nitrogen atoms and a protonated species is related oxygen in the ligands.

In our previous study [17], pyrrolidine linked to 1,2,3-triazole derivatives were examined and dissociation properties of 1,2,3-triazole moieties were explained clearly. The 1,2,3-triazole includes diazinyl group (-N=N-) and tertiary imine nitrogen. While one of two nitrogen atoms in diazinyl groups is very acidic, the other is very basic. Thus, calculated pK_{a1} values (between 2.85 and 3.07) in present study are related to acidic diazinyl nitrogen. Additionally, other diazinyl nitrogen is very basic and it is related to pK_{a3} values (between 10.61 and 10.97). The third nitrogen atom in 1,2,3-triazole ring is the most basic atoms due to electronic effects and related pK_{a5} values varied between 11.01 and 11.54. In present study, proton affinity of nitrogen atoms in the ligands were calculated theoretically using semi-empirical methods such as modified neglect of diatomic overlap (MNDO). The formation heats (H*f*) and the total energies (TE) of the ligands and mono-protonated species were calculated. In addition, the proton affinity of each nitrogen atom (PA) in the ligands was found using formation heats in the following equation and given in Table 3.

$$PA = 367.2 + \Delta H_{f^\circ}(\mathrm{B}) - \Delta H_{f^\circ}(\mathrm{BH}^+)$$

where; PA is the proton affinity of B types; ΔH_{f°(B) is the formation heat of B molecule; $\Delta H_{f^\circ}(BH^+)$ is the formation heat of BH^+ molecule, and 367.2 is the formation heat of H^+ [64].

According to Table 3, the proton affinity of nitrogen in position 3 was higher than the other nitrogen atoms and proton affinity of the nitrogen in position 1 was lower than the others. The nitrogen atom in position 3 was the most basic atom and the most acidic atom was the nitrogen in position 1. Therefore, the first protonated atom was the nitrogen atom in position 3 which present in the molecular structures of the ligands. According to the calculation results, the protonation order for nitrogen atoms in the ligand was as 3 N, 2 N, 4 N and 1 N. Quinoline molecules behave as an aromatic cycle due to delocalization of π electrons. Thus, other two pK_a values (pK_{a2} and pK_{a4}) related to phenolic oxygen and aniline nitrogen atoms. Therefore, attention was paid in this study to explain the pK_a values of 1,4-naphthoquinone-triazole hybrid ligands because of their pharmacological importance.

4. Conclusion

The synthesis of the novel 1,4-naphthoquinone-triazole hybrid compounds **5a–h** containing two very valuable pharmacophore groups was demonstrated and their various biological properties including DNA binding / cleavage, antioxidant and antimicrobial activities were

Table 1
The MIC values (μg/mL) of **5a–h** against the microbial strains (MIC: The minimal inhibitory concentrations).

Compound	*E. coli*	*B. cereus*	*S. aureus*	*P. aeruginosa*	*E. hirae*	*L. pneumophila* subsp. *pneumophila*	*C. albicans*	*C. tropicalis*
5a	128	32	64	32	32	32	64	32
5b	16	8	8	8	16	16	128	64
5c	64	16	16	16	16	16	128	64
5d	32	8	16	8	4	16	32	16
5e	32	16	16	16	4	16	64	32
5f	128	32	32	32	32	16	128	64
5g	128	64	32	32	16	32	64	32
5h	128	16	16	16	16	64	128	64
Ampicillin	0.5	1	1	0.5	0.5	0.5	–	–
Fluconazole	–	–	–	–	–	–	0.5	0.5

Table 2
pK_a values of **5a–h** (20% (*v*/*v*) DMSO-water, 25.0 ± 0.1 °C, I = 0.1 mol/L by NaCl).

Ligand	pK_{a1}	pK_{a2}	pK_{a3}	pK_{a4}	pK_{a5}
5a	2.85 ± 0.01	6.25 ± 0.02	10.43 ± 0.02	10.86 ± 0.01	11.39 ± 0.03
5b	3.06 ± 0.03	5.25 ± 0.02	10.81 ± 0.03	10.99 ± 0.05	11.36 ± 0.07
5c	2.13 ± 0.02	6.66 ± 0.02	10.47 ± 0.02	11.05 ± 0.03	11.46 ± 0.06
5d	2.85 ± 0.01	6.25 ± 0.02	10.43 ± 0.03	10.89 ± 0.03	11.36 ± 0.06
5e	2.60 ± 0.03	6.69 ± 0.03	9.83 ± 0.05	10.38 ± 0.05	11.21 ± 0.08
5f	2.93 ± 0.02	7.07 ± 0.03	10.29 ± 0.03	10.67 ± 0.05	11.17 ± 0.08
5g	3.07 ± 0.01	5.72 ± 0.01	10.39 ± 0.03	10.92 ± 0.02	11.31 ± 0.06
5h	2.71 ± 0.01	7.27 ± 0.02	10.04 ± 0.02	10.68 ± 0.03	11.29 ± 0.047

evaluated in present study. The **5a–h** exhibited high DPPH scavenging and ferrous chelating activities. A form of DNA interaction was apparent due to fluorescence increase for all compounds in the presence of the duplex DNA. While the level of increase was limited up to 2.9 times, this was measured in presence of as low as 1:10 equivalent DNA. Moreover, in spite of the toplogy of the DNA used, dsDNA or G-quadruplex, the fluorescence was enhanced for all tested compounds, **5f**, **5g**, **5h**. This result indicating the potential of these compounds as fluorescent probes; however, fluorescence enhancement may be overshadowed by the DNA cleavage activity. Especially **5c**, **5d**, **5e** and **5h** showed good DNA cleavage activity. All tested compounds displayed antibacterial and antifungal activities. Among all the compounds, **5d** demonstrated the most efficient antimicrobial activity. Present findings on biological activities of the compounds should pass through further pharmacological and toxicological tests and probably will conveniently be used in further antioxidant, antimicrobial and anticancer medicine development.

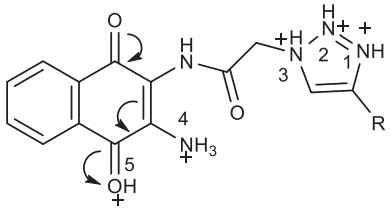

Fig. 7. Full protonated form of the ligands **5a–h** (LH_5^{5+}).

Table 3
The calculated formation heat (H_f), total energy (*TE*) and proton affinity (*PA*) values with MNDO methods for **5a** for symbolized all of the ligands and their mono-protonated forms.

	MNDO		
Species	T.E. (kcal/mol)	Hf (kcal/mol)	PA
5a	−94591.29	−6.50	–
1N-H^+	−94717.18	194.28	166.42
2N-H_2^+	−94756.19	155.27	205.45
3N-H_2^+	−94769.26	142.21	218.49
4N-H_2^+	−94747.62	163.84	196.86

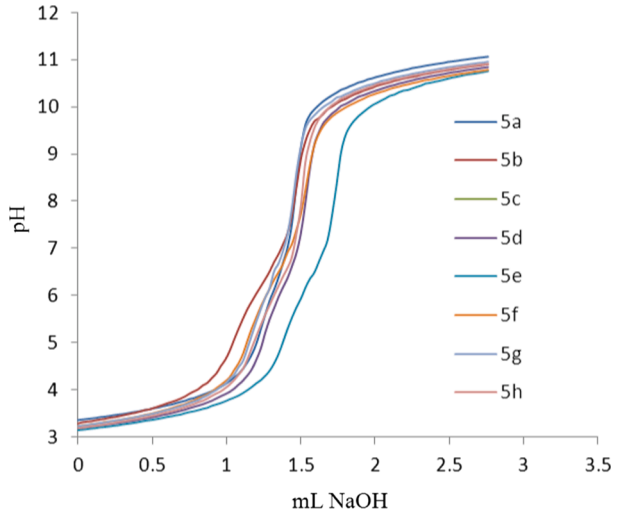

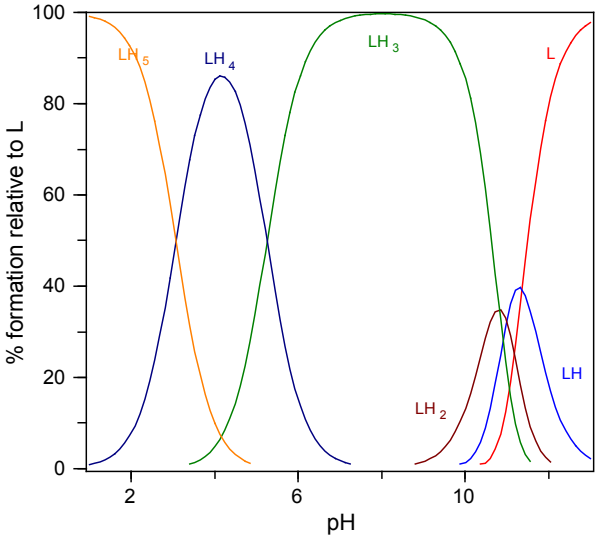

Fig. 6. Titration curves of **5a–h** and distribution curve of **5a** for symbolized all ligands. (25.0 ± 0.1 °C, 0.1 mol/L ionic strength of NaCl in 20% (v/v) DMSO-water).

Further new drug researches are recommended to be performed on such 1,4-naphthoquinone-triazole hybrids. The pK_a values containing critical information about the compounds will provide significant contributions to further pharmacological studies on these types of compounds.

Declaration of Competing Interest

The authors declare no conflict of interest.

Acknowledgements

The authors thank the Scientific and Technological Research Council of Turkey (TÜBİTAK, project grant 119Z033) for financial support.

Appendix A. Supplementary material

Supplementary data to this article can be found online at https://doi.org/10.1016/j.bioorg.2020.104441.

References

[1] H.C. Kolb, M.G. Finn, K.B. Sharpless, Click chemistry: diverse chemical function from a few good reactions, Angew. Chem. Int. Ed. 40 (2001) 2004–2021, https://doi.org/10.1002/1521-3773(20010601)40:11<2004::AID-ANIE2004>3.0.CO;2-5.
[2] A.H. El-Sagheer, T. Brown, Click chemistry with DNA, Chem. Soc. Rev. 39 (2010) 1388–1405, https://doi.org/10.1039/B901971P.
[3] Z. Xu, S.J. Zhao, Y. Liu, 1,2,3-Triazole-containing hybrids as potential anticancer agents: Current developments, action mechanisms and structure-activity relationships, Eur. J. Med. Chem. 183 (2019), 111700, https://doi.org/10.1016/j.ejmech.2019.111700.
[4] X. Jiang, X. Hao, L. Jing, G. Wu, D. Kang, X. Liu, P. Zhan, Recent applications of click chemistry in drug discovery, Expert Opin. Drug Discovery 14 (2019) 779–789, https://doi.org/10.1080/17460441.2019.1614910.
[5] A. Rani, G. Singh, A. Singh, U. Maqbool, G. Kaur, J. Singh, CuAAC-ensembled 1, 2, 3-triazole-linked isosteres as pharmacophores in drug discovery, RSC Adv. 10 (2020) 5610–5635, https://doi.org/10.1039/C9RA09510A.
[6] Y. Teng, Y. Qin, D. Song, X. Liu, Y. Ma, P. Zhang, S. Ma, A novel series of 11-O-carbamoyl-3-O-descladinosyl clarithromycin derivatives bearing 1,2,3-triazole group: Design, synthesis and antibacterial evaluation, Bioorg. Med. Chem. Lett. 30 (2020), 126850, https://doi.org/10.1016/j.bmcl.2019.126850.
[7] F. Gao, L. Ye, F. Kong, G. Huang, J. Xiao, Design, synthesis and antibacterial activity evaluation of moxifloxacin-amide-1,2,3-triazole-isatin hybrids, Bioorg. Chem. 91 (2019), 103162, https://doi.org/10.1016/j.bioorg.2019.103162.
[8] J. Nalawade, A. Shinde, A. Chavan, S. Patil, M. Suryavanshi, M. Modak, P. Choudhari, V.D. Bobade, P.C. Mhaske, Synthesis of new thiazolyl-pyrazolyl-1,2,3-triazole derivatives as potential antimicrobial agents, Eur. J. Med. Chem. 179 (2019) 649–659, https://doi.org/10.1016/j.ejmech.2019.06.074.
[9] W. Tan, Q. Li, H. Wang, Y. Liu, J. Zhang, F. Dong, Z. Guo, Synthesis, characterization, and antibacterial property of novel starch derivatives with 1, 2, 3-triazole, Carbohydr. Polym. 142 (2016) 1–7, https://doi.org/10.1016/j.carbpol.2016.01.007.
[10] S. Srinivasarao, A. Nandikolla, A. Suresh, A.K. Ewa, A. Głogowska, B. Ghosh, B. K. Kumar, S. Murugesan, S. Pulya, H. Aggarwal, K.V.G.C. Sekhar, Discovery of 1, 2, 3-triazole based quinoxaline-1, 4-di-N-oxide derivatives as potential anti-tubercular agents, Bioorg. Chem. 100 (2020), 103955, https://doi.org/10.1016/j.bioorg.2020.103955.
[11] W. Tan, J. Zhang, Y. Mi, F. Dong, Q. Li, Z. Guo, Synthesis, characterization, and evaluation of antifungal and antioxidant properties of cationic chitosan derivative via azide-alkyne click reaction, Int. J. Biol. Macromol. 120 (2018) 318–324, https://doi.org/10.1016/j.ijbiomac.2018.08.111.
[12] W. Tan, J. Zhang, F. Luan, L. Wei, Q. Li, F. Dong, Z. Guo, Synthesis, characterization, and antifungal evaluation of novel 1, 2, 3-triazolium-functionalized starch derivative, Int. J. Biol. Macromol. 101 (2017) 845–851, https://doi.org/10.1016/j.ijbiomac.2017.03.171.
[13] D. González-Calderón, M.G. Mejía-Dionicio, M.A. Morales-Reza, J.G. Aguirre-de Paz, A. Ramírez-Villalva, M. Morales-Rodríguez, A. Fuentes-Benítes, C. González-Romero, Antifungal activity of 1′-homo-N-1, 2, 3-triazol-bicyclic carbonucleosides: A novel type of compound afforded by azide-enolate (3+ 2) cycloaddition, Bioorg. Chem. 69 (2016) 1–6, https://doi.org/10.1016/j.bioorg.2016.09.003.
[14] L. Sun, T. Huang, A. Dick, M.E. Meuser, W.A. Zalloum, C.-H. Chen, X. Ding, P. Gao, S. Cocklin, K.-H. Lee, P. Zhan, X. Liu, Design, synthesis and structure-activity relationships of 4-phenyl-1H-1, 2, 3-triazole phenylalanine derivatives as novel HIV-1 capsid inhibitors with promising antiviral activities, Eur. J. Med. Chem. 190 (2020), 112085, https://doi.org/10.1016/j.ejmech.2020.112085.
[15] T. Manna, K. Pal, K. Jana, A.K. Misra, Anti-cancer potential of novel glycosylated 1, 4-substituted triazolylchalcone derivatives, Bioorg. Med. Chem. Lett. 29 (2019), 126615, https://doi.org/10.1016/j.bmcl.2019.08.019.
[16] S. Li, X.Y. Li, T.J. Zhang, M.O. Kamara, J.W. Liang, J. Zhu, F.H. Meng, Design, synthesis and biological evaluation of homoerythrina alkaloid derivatives bearing a triazole moiety as PARP-1 inhibitors and as potential antitumor drugs, Bioorg. Chem. 94 (2020), 103385, https://doi.org/10.1016/j.bioorg.2019.103385.
[17] T. Ince, R. Serttas, B. Demir, H. Atabey, N. Seferoglu, S. Erdogan, E. Sahin, S. Erat, Y. Nural, Polysubstituted pyrrolidine linked to 1,2,3-triazoles: Synthesis, crystal structure, DFT studies, acid dissociation constant, drug-likeness, and anti-proliferative activity, J. Mol. Struct. 1217 (2020), 128400, https://doi.org/10.1016/j.molstruc.2020.128400.
[18] J. Gour, S. Gatadi, V. Pooladanda, S.M. Ghouse, S. Malasala, Y.V. Madhavi, C. Godugu, S. Nanduri, Facile synthesis of 1, 2, 3-triazole-fused indolo-and pyrrolo [1, 4] diazepines, DNA-binding and evaluation of their anticancer activity, Bioorg. Chem. 93 (2019), 103306, https://doi.org/10.1016/j.bioorg.2019.103306.
[19] J.S. Lv, X.M. Peng, B. Kishore, C.H. Zhou, 1, 2, 3-Triazole-derived naphthalimides as a novel type of potential antimicrobial agents: Synthesis, antimicrobial activity, interaction with calf thymus DNA and human serum albumin, Bioorg. Med. Chem. Lett. 24 (2014) 308–313, https://doi.org/10.1016/j.bmcl.2013.11.013.
[20] R. Gup, O. Erer, N. Dilek, One-pot synthesis of a new 2-substituted 1, 2, 3-triazole 1-oxide derivative from dipyridyl ketone and isonitrosoacetophenone hydrazone: Nickel (II) complex, DNA binding and cleavage properties, Bioorg. Chem. 71 (2017) 325–334, https://doi.org/10.1016/j.bioorg.2017.03.003.
[21] S. Narsimha, N.S. Kumar, B.K. Swamy, N.V. Reddy, S.A. Hussain, M.S. Rao, Indole-2-carboxylic acid derived mono and bis 1, 4-disubstituted 1,2,3-triazoles: synthesis, characterization and evaluation of anticancer, antibacterial, and DNA-cleavage activities, Bioorg. Med. Chem. Lett. 26 (2016) 1639–1644, https://doi.org/10.1016/j.bmcl.2016.01.055.
[22] Y. Chen, X. Liu, X. Sun, J. Zhang, Y. Mi, Q. Li, Z. Guo, Synthesis and antioxidant activity of cationic 1, 2, 3-triazole functionalized starch derivatives, Polymers 12 (2020) 112, https://doi.org/10.3390/polym12010112.
[23] G. Singh, A. Arora, P. Kalra, I.K. Maurya, C.E. Ruizc, M.A. Estebanc, S. Sinha, K. Goyal, R. Sehgale, A strategic approach to the synthesis of ferrocene appended chalcone linked triazole allied organosilatranes: antibacterial, antifungal, antiparasitic and antioxidant studies, Bioorgan. Med. Chem. 27 (2019) 188–195, https://doi.org/10.1016/j.bmc.2018.11.038.
[24] W. Tan, J. Zhang, X. Zhao, F. Dong, Q. Li, Z. Guo, Synthesis and antioxidant action of chitosan derivatives with amino-containing groups via azide-alkyne click reaction and N-methylation, Carbohydr. Polym. 199 (2018) 583–592, https://doi.org/10.1016/j.carbpol.2018.07.056.
[25] M. Yazdani, N. Edraki, R. Badri, M. Khoshneviszadeh, A. Iraji, O. Firuzi, Multi-target inhibitors against Alzheimer disease derived from 3-hydrazinyl 1, 2, 4-triazine scaffold containing pendant phenoxy methyl-1, 2, 3-triazole: Design, synthesis and biological evaluation, Bioorg. Chem. 84 (2019) 363–371, https://doi.org/10.1016/j.bioorg.2018.11.038.
[26] M.L. Macías-Rubalcava, M.E.R.V. Sobrino, C. Melendez-Gonzalez, B. King-Diaz, B. Lotina-Hennsen, Selected phytotoxins and organic extracts from endophytic fungus *Edenia gomezpompae* as light reaction of photosynthesis inhibitors, J. Photoch. Photobio. B 138 (2014) 17–26, https://doi.org/10.1016/j.jphotobiol.2014.05.003.
[27] D. Aminin, S. Polonik, 1,4-Naphthoquinones: Some biological properties and application, Chem. Pharm. Bull. 68 (2020) 46–57, https://doi.org/10.1248/cpb.c19-00911.
[28] K. Li, B. Wang, L. Zheng, K. Yang, Y. Li, M. Hu, D. He, Target ROS to induce apoptosis and cell cycle arrest by 5, 7-dimethoxy-1,4-naphthoquinone derivative, Bioorg. Med. Chem. Lett. 28 (2018) 273–277, https://doi.org/10.1016/j.bmcl.2017.12.059.
[29] M. Gemili, Y. Nural, E. Keleş, B. Aydıner, N. Seferoğlu, M. Ülger, E. Şahin, S. Erat, Z. Seferoğlu, Novel highly functionalized 1, 4-naphthoquinone 2-iminothiazole hybrids: synthesis, photophysical properties, crystal structure, DFT studies, and anti(myco) bacterial/antifungal activity, J. Mol. Struct. 1196 (2019) 536–546, https://doi.org/10.1016/j.molstruc.2019.06.087.
[30] A. Defant, A. Vozza, I. Mancini, Design, synthesis and antimicrobial evaluation of new norfloxacin-naphthoquinone hybrid molecules, Proceedings 41 (2019) 9. https://doi.org/10.3390/ecsoc-23-06480.
[31] A.F. Tuyun, M. Yıldız, N. Bayrak, H. Yıldırım, E. Mataracı Kara, A.T. Jannuzzi, B. Ozbek Celik, Discovery of a new family of heterocyclic amine linked plastoquinone analogs for antimicrobial evaluation, Drug Devel. Res. 80 (2019) 1098–1109, https://doi.org/10.1002/ddr.21591.
[32] F.R.F. Dias, J.S. Novais, T.A.D.N.S. Devillart, W.A. da Silva, M.O. Ferreira, R.B. S. Loureiro, V.R. Campos, V.F. Ferreira, M.C.B.V. de Souza, H.C. Castro, A. C. Cunha, Synthesis and antimicrobial evaluation of amino sugar-based naphthoquinones and isoquinoline-5, 8-diones and their halogenated compounds, Eur. J. Med. Chem. 156 (2018) 1–12, https://doi.org/10.1016/j.ejmech.2018.06.050.
[33] M. Janeczko, O.M. Demchuk, D. Strzelecka, K. Kubiński, M. Masłyk, New family of antimicrobial agents derived from 1, 4-naphthoquinone, Eur. J. Med. Chem. 124 (2016) 1019–1025, https://doi.org/10.1016/j.ejmech.2016.10.034.
[34] J.P. Shrestha, C. Baker, Y. Kawasaki, Y.P. Subedi, N.N.V. de Paul, J.Y. Takemoto, C. W.T. Chang, Synthesis and bioactivity investigation of quinone-based dimeric cationic triazolium amphiphiles selective against resistant fungal and bacterial pathogens, Eur. J. Med. Chem. 126 (2017) 696–704, https://doi.org/10.1016/j.ejmech.2016.12.008.
[35] E.O. Olawode, R. Tandlich, E. Prinsloo, M. Isaacs, H. Hoppe, R. Seldon, D. F. Warner, V. Steenkamp, P.T. Kaye, Synthesis and biological evaluation of 2-chloro-3-[(thiazol-2-yl) amino]-1,4-naphthoquinones, Bioorg. Med. Chem. Lett. 29 (2019) 1572–1575, https://doi.org/10.1016/j.bmcl.2019.05.001.
[36] T. Kundu, A. Pramanik, Expeditious and eco-friendly synthesis of new multifunctionalized pyrrole derivatives and evaluation of their antioxidant

property, Bioorg. Chem. 98 (2020), 103734, https://doi.org/10.1016/j.bioorg.2020.103734.
[37] K. Mathiyazhagan, A. Kumaran, P. Arjun, Isolation of natural naphthoquinones from *Juglans regia* and in vitro antioxidant and cytotoxic studies of naphthoquinones and the synthetic naphthofuran derivatives, Russ. J. Bioorg. Chem. 44 (2018) 346–353, https://doi.org/10.1134/S1068162018030111.
[38] A.A. Aly, E.M. El-Sheref, M.E. Bakheet, M.A. Mourad, A.B. Brown, S. Bräse, M. Nieger, M.A. Ibrahim, Synthesis of novel 1, 2-bis-quinolinyl-1, 4-naphthoquinones: ERK2 inhibition, cytotoxicity and molecular docking studies, Bioorg. Chem. 81 (2018) 700–712, https://doi.org/10.1016/j.bioorg.2018.09.017.
[39] N. Bayrak, H. Yıldırım, A.F. Tuyun, E. Mataraci Kara, B. Ozbek Celik, G. Kumar Gupta, I.H. Ciftci, M. Fujita, M. Otsuka, H.R. Nasiri, Synthesis, computational study, and evaluation of in vitro antimicrobial, antibiofilm, and anticancer activities of new sulfanyl aminonaphthoquinone derivatives, Lett. Drug Des, Discovery 14 (2017) 647–661, https://doi.org/10.2174/1570180814061706061555530.
[40] A. Kosiha, C. Parthiban, K.P. Elango, Synthesis, characterization and DNA binding/cleavage, protein binding and cytotoxicity studies of Co (II), Ni (II), Cu (II) and Zn (II) complexes of aminonaphthoquinone, J. Photoch. Photobio. B 168 (2017) 165–174, https://doi.org/10.1016/j.jphotobiol.2017.02.010.
[41] A. Kosiha, C. Parthiban, S. Ciattini, L. Chelazzi, K.P. Elango, Metal complexes of naphthoquinone based ligand: Synthesis, characterization, protein binding, DNA binding/cleavage and cytotoxicity studies, J. Biomol. Struct. Dyn. 36 (2018) 4170–4181, https://doi.org/10.1080/07391102.2017.1413423.
[42] M. Gholampour, S. Ranjbar, N. Edraki, M. Mohabbati, O. Firuzi, M. Khoshneviszadeh, Click chemistry-assisted synthesis of novel aminonaphthoquinone-1,2,3-triazole hybrids and investigation of their cytotoxicity and cancer cell cycle alterations, Bioorg. Chem. 88 (2019) 102967, https://doi.org/10.1016/j.bioorg.2019.102967.
[43] S.F. Vasilevsky, D.S. Baranov, A.I. Govdi, I.V. Sorokina, T.G. Tolstikova, G. A. Tolstikov, I.V. Alabugin, Click chemistry on diterpenes: anti-inflammatory activity of the acetylenic derivatives of levopimaric acid and products of their transformations, Arkivoc 2014 (2014) 145–157, https://doi.org/10.3998/ark.5550190.p008.471.
[44] E.B.T. Diogo, G.G. Dias, B.L. Rodrigues, T.T. Guimarães, W.O. Valença, C. A. Camara, R.N. de Oliveira, M.G. da Silva, V.F. Ferreira, Y.G. de Paiva, M.O. F. Goulart, R.F.S. Menna-Barreto, S.L.E.N. de Castroda Silva Júnior, Synthesis and anti-*Trypanosoma cruzi* activity of naphthoquinone-containing triazoles: Electrochemical studies on the effects of the quinoidal moiety, Bioorgan. Med. Chem. 21 (2013) 6337–6348, https://doi.org/10.1016/j.bmc.2013.08.055.
[45] T.T. Guimarães, M.D.C.F.R. Pinto, J.S. Lanza, M.N. Melo, R.L. do Monte-Neto, I.M. M. de Melo, E.B.T. Diogo, V.F. Ferreira, C.A. Camara, W.O. Valença, R.N. de Oliveira, F. Frézard, E.N. da Silva Júnior, Potent naphthoquinones against antimony-sensitive and-resistant Leishmania parasites: Synthesis of novel α-and nor-α-lapachone-based 1,2,3-triazoles by copper-catalyzed azide–alkyne cycloaddition, Eur. J. Med. Chem. 63 (2013) 523-530. https://doi.org/10.1016/j.ejmech.2013.02.038.
[46] B.D. Bala, S. Muthusaravanan, T.S. Choon, M.A. Ali, S. Perumal, Sequential synthesis of amino-1,4-naphthoquinone-appended triazoles and triazole-chromene hybrids and their antimycobacterial evaluation, Eur. J. Med. Chem. 85 (2014) 737–746, https://doi.org/10.1016/j.ejmech.2014.08.009.
[47] J. Lee, H. Kim, M.J. Park, Long-life, high-rate lithium-organic batteries based on naphthoquinone derivatives, Chem. Mater. 28 (2016) 2408–2416, https://doi.org/10.1021/acs.chemmater.6b00624.
[48] M. Gemili, Y. Nural, E. Keleş, B. Aydıner, N. Seferoğlu, E. Şahin, H. Sarı, Z. Seferoğlu, Novel 1,4-naphthoquinone N-aroylthioureas: Syntheses, crystal structure, anion recognition properties, DFT studies and determination of acid dissociation constants, J. Mol. Liq. 269 (2018) 920–932, https://doi.org/10.1016/j.molliq.2018.08.054.
[49] J.L. Wang, Y.G. Zhao, B.S. Yang, Transition metal complexes of asymmetrical aroyl-hydrazone ligand: Syntheses, structures, DNA binding and cleavage studies, Inorg. Chim. Acta 409 (2014) 484–496, https://doi.org/10.1016/j.ica.2013.09.001.
[50] M.S. Blois, Antioxidant determinations by the use of a stable free radical, Nature 181 (1958) 1199–1200, https://doi.org/10.1038/1811199a0.
[51] T.C.P. Dinis, V.M.C. Madeira, L.M. Almeida, Action of phenolic derivates (acetoaminophen, salycilate and 5-aminosalycilate) as inhibitors of membrane lipid peroxidation and as peroxyl radical scavengers, Arch. Biochem. Biophy. 315 (1994) 161–169, https://doi.org/10.1006/abbi.1994.1485.
[52] Y. Nural, M. Gemili, E. Yabalak, L.M. De Coen, M. Ulger, Green synthesis of highly functionalized octahydropyrrolo[3, 4-c]pyrrole derivatives using subcritical water, and their anti(myco)bacterial and antifungal activity, Arkivoc 5 (2018) 51–64. https://doi.org/10.24820/ark.5550190.p010.573.
[53] A. Braibanti, G. Ostacoli, P. Paoletti, L.D. Pettit, S. Sammartano, Recommended procedure for testing the potentiometric apparatus and technique for the pH-metric measurement of metal-complex equilibrium constants, Pure Appl. Chem. 59 (1987) 1721–1728, https://doi.org/10.1351/pac198759121721.
[54] Y. Nural, M. Gemili, N. Seferoglu, E. Sahin, M. Ulger, H. Sari, Synthesis, crystal structure, DFT studies, acid dissociation constant, and antimicrobial activity of methyl 2-(4-chlorophenyl)-7a-((4-chlorophenyl)carbamothioyl)-1-oxo-5,5-diphenyl-3-thioxo-hexahydro-1H-pyrrolo[1,2-e] imidazole-6-carboxylate, J. Mol. Struct. 1160 (2018) 375–382, https://doi.org/10.1016/j.molstruc.2018.01.099.
[55] Y. Nural, Synthesis, antimycobacterial activity, and acid dissociation constants of polyfunctionalized 3-[2-(pyrrolidin-1-yl)thiazole-5-carbonyl]-2H-chromen-2-one derivatives, Monatsh. Chem. 149 (2018) 1905–1918, https://doi.org/10.1007/s00706-018-2250-7.
[56] Y. Nural, M. Gemili, M. Ulger, H. Sari, L.M. De Coen, E. Sahin, Synthesis, antimicrobial activity and acid dissociation constants of methyl 5,5-diphenyl-1-(thiazol-2-yl) pyrrolidine-2-carboxylate derivatives, Bioorg. Med. Chem. Lett. 28 (2018) 942–946, https://doi.org/10.1016/j.bmcl.2018.01.045.
[57] E. Niki, Antioxidants in relation to lipid peroxidation, Chem. Phys. Lipids 44 (1987) 227–253, https://doi.org/10.1016/0009-3084(87)90052-1.
[58] R. Sudan, M. Bhagat, S. Gupta, J. Singh, A. Koul, Iron (FeII) chelation, ferric reducing antioxidant power, and immune modulating potential of *Arisaema jacquemontii* (Himalayan Cobra Lily), BioMed. Res. Int. 2014 (2014), 179865, https://doi.org/10.1155/2014/179865.
[59] M.A. Ebrahimzadeh, F. Pourmorad, A.R. Bekhradnia, Iron chelating activity, phenol and flavonoid content of some medicinal plants from Iran, Afr. J. Biotechnol. 7 (2008) 3188–3192, https://doi.org/10.5897/AJB08.476.
[60] V.T. Aparadh, V.V. Naik, B.A. Karadge, Antioxidative properties (TPC, DPPH, FRAP, metal chelating ability, reducing power and TAC) within some Cleome species, Annali di Botanica 2 (2012) 49–56, https://doi.org/10.4462/annbotrm-9958.
[61] N. Zhang, S. Ma, Recent development of membrane-active molecules as antibacterial agents, Eur. J. Med. Chem. 184 (2019), 111743, https://doi.org/10.1016/j.ejmech.2019.111743.
[62] K. Mazák, B. Noszál, Advances in microspeciation of drugs and biomolecules: species-specific concentrations, acid-base properties and related parameters, J. Pharmaceut. Biomed. 130 (2016) 390–403, https://doi.org/10.1016/j.jpba.2016.03.053.
[63] M. Gemili, H. Sari, M. Ulger, E. Sahin, Y. Nural, Pt (II) and Ni (II) complexes of octahydropyrrolo[3,4-c]pyrrole N-benzoylthiourea derivatives: Synthesis, characterization, physical parameters and biological activity, Inorg. Chim. Acta 463 (2017) 88–96, https://doi.org/10.1016/j.ica.2017.04.026.
[64] M.J. Dewar, K.M. Dieter, Evaluation of AM1 calculated proton affinities and deprotonation enthalpies, J. Am. Chem. Soc. 108 (1986) 8075–8086, https://doi.org/10.1021/ja00285a033.